Assessing Viscosity and Contaminant Levels in Diesel Lubricant through Dielectric Spectroscopy Utilizing Soft Computing Approaches

M. R. Pourramezan[1], A. Rohani[1*], M. H. Abbaspour-Fard[1]

1- Department of Biosystems Engineering, Faculty of Agriculture, Ferdowsi University of Mashhad, Mashhad, Iran
(*- Corresponding Author Email: arohani@um.ac.ir)
https://doi.org/10.22067/jam.2025.91756.1335

Abstract

Monitoring the status of machinery is a crucial aspect of production and service units to uphold operational efficiency. Timely changes in engine lubricant significantly contribute to enhanced performance and extended engine lifespan. However, determining the precise replacement time remains a challenge. Oil spectral analysis, while effective, is both expensive and time-intensive. This study aims to introduce an alternative method to engine lubricant spectral analysis. The investigation involves analyzing the results of spectral analysis and dielectric coefficients of 17 engine lubricant samples through statistical methods. The primary objective is to develop models for predicting oil contaminants based on dielectric properties, offering a substitute for spectral analysis. To achieve this, several intermediate goals are pursued. Multilayer perceptron artificial neural networks (MLP-ANN) and support vector machine (SVM) methods are employed for modeling. The performance of the two models is assessed using indicators such as Root Mean Square Error (RMSE), model efficiency, and R-squared (R^2). The results indicate that the SVM model consistently demonstrates an efficiency exceeding 0.95 for all predicted indices (Fe, Pb, Cu, Al, Mo, Na, Si, and Vis@100). Consequently, dielectric spectroscopy of lubricant emerges as a viable alternative to traditional oil spectral analysis.

Keywords: Dielectric constant, Engine lubricant condition monitoring, Metrology, Soft computing methods

Abbreviations

ASTM	American Society for Testing and Materials	DS	Dielectric spectroscopy
E	Efficiency	FTIR	Fourier transform infrared
GA	Genetic algorithm	ISM	Industrial, Scientific and Medical
MLP	Multilayer Perceptron	MAPE	Mean absolute percentage error
NN	Neural network	R^2	Coefficient of determination
RBF	Radial basis function	RFE	Recursive feature elimination
RMSE	Root means square error	SA	Spectral Analysis
SC	Soft computing	SVM	Support vector machine
TAN	Total acid number	VNA	Vector network analyzer

Introduction

Condition monitoring, a cornerstone of predictive maintenance, plays a pivotal role in anticipating equipment failures, safeguarding safety, and adhering to regulatory requirements (Mosher, 2007). This is particularly crucial for complex systems, where a comprehensive assessment of operational parameters and human inspection findings is essential for evaluating equipment performance and identifying anomalous conditions (Pourramezan, Rohani, Keramat Siavash, & Zarein, 2022). As illustrated in Figure 1, the evolution of maintenance strategies has transitioned from reactive approaches to proactive methods, including preventive and condition-based maintenance. This transformation has yielded substantial advancements in safety, reliability, and cost-effectiveness across diverse industries such as manufacturing, transportation, agriculture, and energy production (Lazakis, Raptodimos, & Varelas, 2018; Pourramezan, Rohani, & Abbaspour-Fard, 2023b).

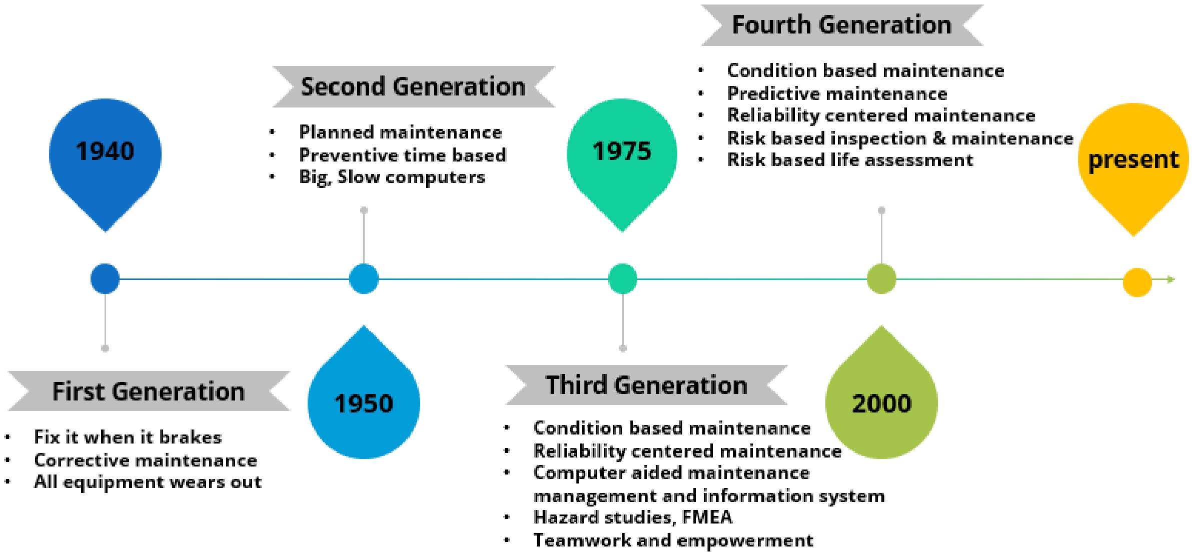

Fig. 1. Evolution of maintenance strategies: a shift from reactive to proactive approaches (Pourramezan *et al.*, 2023b)

Engine lubricants play a multitude of crucial roles in optimizing engine performance (Zhu, Zhong, & Zhe, 2017). These lubricants effectively reduce friction and wear between moving components, facilitate heat transfer and energy distribution, prevent corrosion, and cleanse the internal engine compartments (Kim, Seo, Kang, & Kim, 2016; Mondelin, Claudin, Rech, & Dumont, 2011; Zhu, Wang, Luo, Zhang, & Liu, 2022). However, engine lubricants degrade over time, particularly at elevated temperatures, significantly impacting their tribological performance. This degradation manifests as a reduction in lubricant viscosity, base number (BN), and flash point, accompanied by the formation of detrimental substances such as heavy metals and polycyclic aromatic hydrocarbons (PAHs) (Heredia-Cancino, Ramezani, & Álvarez-Ramos, 2018; Zzeyani, Mikou, & Naja, 2018). traditional machinery maintenance practices often involve monitoring lubricant levels and replacing lubricants based on mileage schedules. However, this "quantity-based" approach is no longer sufficient to ensure optimal lubrication performance and minimize power losses and maintenance costs. The development of advanced engine oil monitoring systems is essential for assessing lubricant degradation and maintaining lubrication effectiveness (Pourramezan, Rohani, & Abbaspour-Fard, 2025). Numerous sensors and systems have been developed by scientists and specialists for monitoring one or more of an engine's performance parameters (Hong & Jeon, 2022). These systems employ a diverse range of techniques, including electrical (magnetic), physical, chemical, and optical methods (Zhu *et al.*, 2017). However, monitoring chemical changes in hydraulic oils and lubricants remains challenging due to the limitations of laboratory-based techniques for real-time industrial applications (Duchowski & Mannebach, 2006). The adoption of low-cost condition monitoring techniques offers significant practical benefits and economic advantages (Woodley, 1978; You, Liu, & Meng, 2011). Additionally, continuous monitoring of error patterns and parameter variations is crucial for fault diagnosis and condition-based maintenance (Bhattacharya & Dan, 2014).

Presence of contaminants, both solid and liquid particles, can lead to premature bearing wear and performance degradation (Pourramezan *et al.*, 2022). Studies have demonstrated that contamination and physical changes significantly impact lubricant performance, invariably altering the lubricant's dielectric constant (Pourramezan *et al.*, 2023b; Raadnui & Kleesuwan, 2005). The dielectric constant, a crucial indicator of oil aging, is also influenced by factors such as base oil type, additives, temperature, and electric field frequency (Chun, 2006; Gomółka & Augustynowicz, 2019). Published research has established a strong correlation between increased lubricant operating hours, oil sample degradation, and an increase in dielectric constant. In essence, determining the dielectric constant of an oil sample can provide insights into the lubricant's degradation rate. Studies have confirmed that extended oil operating hours lead to further degradation and an elevated dielectric constant (Altıntaş, Aksoy, Ünal, Akgöl, & Karaaslan, 2019). Researchers have employed dielectric spectroscopy to investigate engine lubricant oxidation and determine total acid number (TAN). Their findings, compared to Fourier transform infrared (FTIR) results, demonstrate the effectiveness of both methods in monitoring lubricant condition (Guan, Feng, Xiong, & Xie, 2011). One study has proposed a methodology for locomotive system maintenance. This research investigated the relationship between dielectric properties and metallic and non-metallic particles, including iron (Fe), aluminum (Al), chromium (Cr), lead (Pb), copper (Cu), zinc (Zn), and silicon (Si). Artificial neural networks were employed to explore the correlation between dielectric constant, dielectric loss factor, and oil impurities. The highest regression values (R) were obtained for the dielectric constant and dielectric loss factor at 7.4 GHz, with values of 0.8513 and 0.8015, respectively (Altıntaş *et al.*, 2019). Dielectric or impedance spectroscopy, a non-destructive technique, offers numerous advantages for researchers and engineers. Not only is it a cost-effective method, but it also provides valuable insights into the electrical behavior of materials (Gerhardt, 2022; Sapotta, Schwotzer, Wöll, & Franzreb, 2022).

Fuzzy logic techniques and artificial neural networks (ANNs) have emerged as valuable tools for data analysis in the context of position analysis and equipment troubleshooting within autonomous monitoring systems for industrial equipment (Li, Fei, & Zhang, 2022). Recognizing the importance of reliability, safety, optimal machinery utilization, and the intricate nature of maintenance challenges, researchers have turned to soft computing methodologies for lubrication status monitoring (Król, Gocman, & Giemza, 2015; Li, Chang, Zhou, & Xiao, 2017). Researchers have developed a support vector machine (SVM)-based model to identify and forecast external wear failures based on oil condition monitoring data. This study employed recursive feature elimination (RFE) to reduce independent variables within the model. The highest achieved accuracy in this work was 94.20%. The findings revealed that iron, aluminum, and lead are crucial factors in determining diesel engine erosion status (Li *et al.*, 2017). Yu *et al.* proposed a method for diagnosing oil pump failures using radial basis function (RBF) neural networks (NNs) in conjunction with a genetic algorithm (GA). Their results demonstrated that the proposed model achieved an accuracy exceeding 96% (Yu, Zhao, Chen, & Hou, 2016). Sanga *et al.* employed an RBF neural network to classify breakdowns based on information obtained from the car engine's airway. Their findings indicated that the RBF model could classify failures with an error rate of 2% (Sangha, Gomm, & Yu, 2008).

A soft computing-based method (KNN and RBF-ANN) was developed to evaluate engine health using a reduced set of lubricant parameters, reducing testing costs. Analyzing 681 engine lubricant reports identified seven key indicators—iron, chromium, lead, copper, aluminum, nickel, and time depending on the particle quantifier (TDPQ)—that significantly impacted distinguishing between normal, caution, and critical wear stages. Both models exhibited high accuracy and sensitivity, with the RBF-ANN achieving an accuracy of approximately 99.85% across all three training set sizes (40%, 60%, and 80%). Overall, the findings suggest that soft computing methods can accurately diagnose engine health using a minimized set of indicators (Pourramezan *et al.*, 2022). The impact of metal and non-metal contaminants on diesel engine conditions was investigated using Support Vector Machines (SVM) and Radial Basis Function (RBF) models. Among the models tested, RBF demonstrated the best generalization performance across varying dataset sizes (10% to 90%). The study also identified key metal contaminants, such as Cr, Si, and Fe, that significantly influenced engine identification in normal and critical states. The confusion matrix approach of RBF-NN achieved an accuracy of 99.38% in diagnosing the critical state of the engine (Rahimi, Pourramezan, & Rohani, 2022). The feasibility of using soft computing models to predict elemental spectroscopy of engine lubricants based on their electrical properties was explored. A dataset of 49 lubricant samples, including elemental spectroscopy and dielectric properties, was utilized to train and test models such as RBF, ANFIS, SVM, MLP, and GPR. The RBF model consistently provided the most accurate predictions for silicon at 7.4 GHz, with root mean squared error (RMSE) and mean absolute percentage error (MAPE) values of 0.4 and 0.7, respectively (Pourramezan *et al.*, 2023b). The potential of soft computing models for predicting the viscosity of used engine lubricant based on oil analysis results was evaluated. A dataset of 555 engine oil analysis reports related to two types of oils (15W40 and 20W50) was employed. Six models, including SVM, ANFIS, GPR, MLR, MLP, and RBF, were developed and assessed for viscosity prediction. The RBF model demonstrated superior accuracy, consistency, and generalizability compared to the other models, achieving RMSE values of 0.20 during training and 0.11 during testing, and efficiency (EF) values of 0.99 during training and 1 during testing (Pourramezan, Rohani, & Abbaspour-Fard, 2023a).

In this work, we propose a novel approach to evaluating engine oil condition by employing dielectric spectroscopy (DS) as a non-invasive and cost-effective alternative to conventional spectral analysis (SA). DS measures the dielectric properties of oil over a wide range of frequencies, providing a wealth of data for developing robust soft computing (SC) models that accurately predict oil indices. Our research utilizes lubricant samples extracted directly from engines, ensuring the relevance of our findings to real-world conditions and enhancing their applicability. Despite the limited sample size, we believe our work serves as a promising proof-of-concept and paves the way for future validation on an industrial scale. The wide frequency range employed (300 MHz to 9 GHz) further enriches the data available for modeling, enabling deeper insights into oil degradation and performance. Additionally, our method holds the potential to significantly reduce the cost and time associated with engine oil spectral analysis, overcoming the limitations inherent in current monitoring practices.

Materials and Methods

The study was carried out in three distinct phases, as depicted in Figure 2.

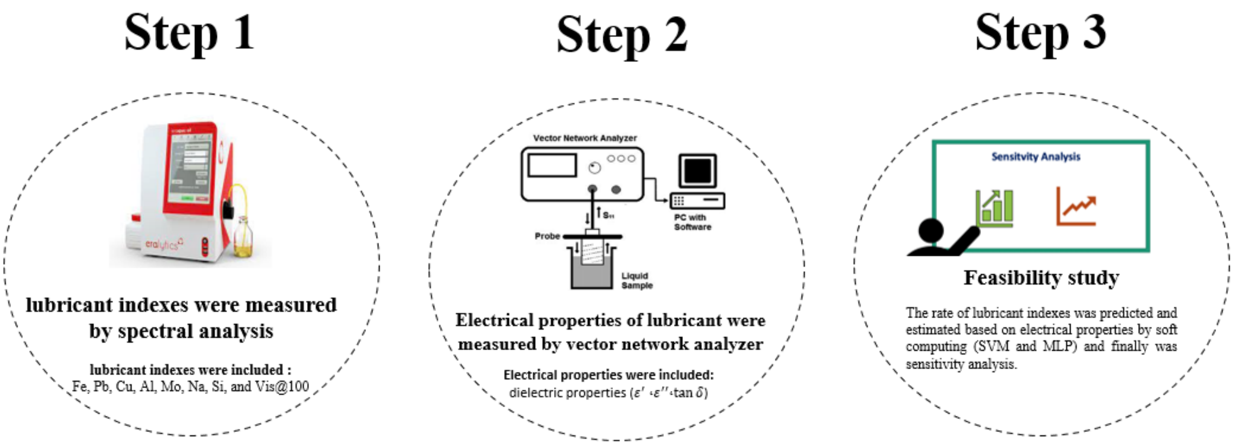

Fig. 2. Research general process flow chart

Spectral analysis method

The study initially employed spectral analysis (SA) to characterize the diesel engine lubricants. Oil analysis involves measuring viscosity, acidity, wear, and metal contamination through spectroscopy (Macián, Tormos, Olmeda, & Montoro, 2003; Newell, 1999). Sixteen diesel engine lubricant samples were obtained from various machines (road construction machines, mainly dump trucks). The oil grade (20W50) and engine type (TYM T2300T3) were identical for all samples. All the machines were property of the Tirage Company in Iran. The concentrations of Fe, Pb, Cu, Al, Mo, Na, and Si were determined according to ASTM D6595. Additionally, the viscosity at 100°C (Vis@100) was determined according to ASTM D445. One sample of fresh 20W50 lubricant was prepared for a more comprehensive study. Measurements were conducted at the commercial laboratory of Tavan Kav Net in Iran. All results are presented in Table 1.

Table 1- The results of spectral analysis on lubricant samples

Sample NO.	Oil Hours	Fe	Pb	Cu	Al	Mo	Na	Si	Vis@100
		Unit: PPM							Unit: Cst
1	100	11.05	0.98	2.83	3.62	48.68	3.46	8.79	16.23
2	150	9.94	0.97	0	1.61	46.11	2.56	17.77	15.3
3	50	30.25	1.64	0	10.18	50.36	8.99	9.23	20.03
4	80	81.17	2.59	0	34.59	52.23	9.32	36.21	15.94
5	100	13.19	0.59	1.8	1.09	36.24	2.33	7.14	15.99
6	160	24.65	1.25	0	5.05	48.78	3.81	9.89	16.35
7	130	9.24	0.92	0	1	45.75	2.86	6.11	15.33
8	160	15.46	1.75	0	0.38	45.81	2.31	4.01	15.02
9	100	39	7.78	4.42	10.93	28.84	9.99	16.29	17.5
10	100	39.76	1.4	3.2	3.77	77.64	13.67	15.44	17.83
11	70	34.69	1.23	0.18	13.45	37.75	4.15	16.55	17.81
12	150	39.67	2.31	3.91	12.45	46.98	5.32	16.33	17.59
13	50	86.06	2.76	1.17	10.95	52.53	3.46	40.05	18.64
14	74	21.73	7.23	3.22	5.31	40.78	3.89	7.27	15.33
15	100	8.17	3.23	1.79	0	26.86	1.2	7.22	7.85
16	100	49.75	4.11	3.51	5.07	12.16	9.57	13.65	13.67
17 (Fresh oil)	0	0	0	0	0	0	0	0	22

Measurement of dielectric properties

The second step involved measuring the dielectric properties of all 17 lubricant samples (16 used and one fresh) at various frequency points. Every material in nature possesses fundamental electrical parameters, including permittivity, permeability, and conductivity. Permittivity exhibits both real and imaginary components, and their relationship with the dielectric constant is defined by Equation (1) (Altıntaş *et al.*, 2019):

$$k = \varepsilon^* = \varepsilon' - j\varepsilon'' \tag{1}$$

where k is the dielectric constant, also known as relative permittivity (ε^*). ε' represents the real part of the dielectric constant, while ε'' denotes the imaginary part. The symbol j represents the imaginary unit $\sqrt{-1}$.

The dielectric constant of a material quantifies its ability to store electrical energy relative to free space. However, it can vary under different conditions, such as frequency, temperature, composition, and pressure (Mumby, 1989;

Zeng, Zhang, Zhang, & Hu, 2010). The real part of the dielectric constant, ε', reflects a material's ability to store electrical energy when subjected to an electromagnetic field. The imaginary part, ε", indicates the dissipation of electromagnetic energy in the material. The loss coefficient, $\tan\delta$, quantifies the conversion of electromagnetic energy into heat and is calculated using Equation (2) (Pourramezan, Rohani, & Abbaspour-Fard, 2024):

$$\tan\delta = \frac{\varepsilon''}{\varepsilon'} \tag{2}$$

In this study, a wide frequency band was employed to measure the dielectric properties. Furthermore, the probe reflectance method was employed to monitor the environmental state (Pourramezan *et al.*, 2023b). This method involves determining the dielectric properties of lubricant samples by comparing the amplitude and phase values of the reflected wave with the radiated wave (Zarein, Khoshtaghaza, & Ameri Mahabadi, 2019). The dielectric properties (ε', ε", $\tan\delta$) of the lubricant samples were measured using an R&S ZVL 13 vector network analyzer (VNA) manufactured in the USA. This VNA can accurately analyze microwave absorbing properties in the 9 kHz to 13.6 GHz frequency range with ±0.2 dB accuracy (see Fig.3).

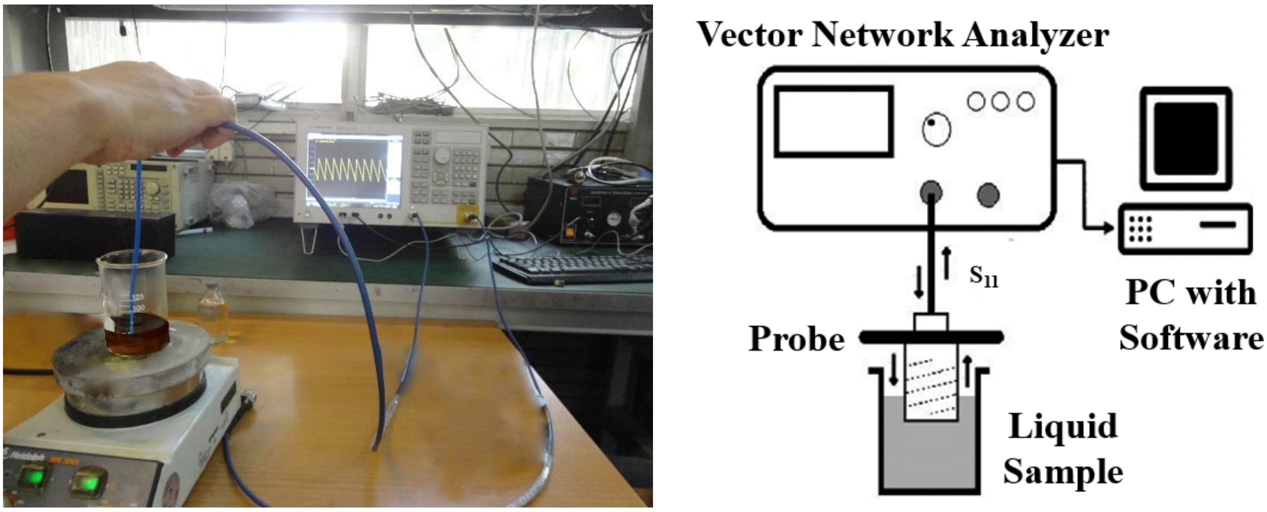

Fig. 3. Experimental and schematic setup for dielectric properties measurement

As shown in Figure 3, 50 ml of each lubricant sample was poured into a beaker, and a coaxial dielectric probe was inserted into the oil sample. Initially, the frequencies of 434, 915, 2450, and 5800 MHz were considered, corresponding to industrial, scientific, and medical (ISM) frequencies (Nüchter, Ondruschka, Bonrath, & Gum, 2004). Subsequently, appropriate frequency points were determined within each frequency range. Finally, the measurements were conducted at 40 frequency points distributed across the 300 MHz to 9 GHz frequency range (Table 2). The measurements for each sample were repeated three times under identical conditions to ensure consistency and accuracy.

Table 2- Frequency points used in the 300 MHz to 9 GHz frequency range

Symbol	Frequency (GHz)	Symbol	Frequency (GHz)	Symbol	Frequency (GHz)	Symbol	Frequency (GHz)
f1	0.3	f11	2.45	f21	4.6895	f31	6.9495
f2	0.434	f12	2.6	f22	4.9155	f32	7.1755
f3	0.675	f13	2.84	f23	5.1415	f33	7.4015
f4	0.915	f14	3.085	f24	5.3675	f34	7.6275
f5	1.16	f15	3.325	f25	5.5935	f35	7.8535
f6	1.4	f16	3.565	f26	5.8195	f36	8.0795
f7	1.64	f17	3.8	f27	6.0455	f37	8.3055
f8	1.88	f18	4	f28	6.2715	f38	8.5315
f9	2.12	f19	4.2375	f29	6.4975	f39	8.7575
f10	2.36	f20	4.4635	f30	6.7235	f40	9

Design of soft computing models

This section explores the application of soft computing models to predict the values of oil analysis indices (Section 2.1) from their dielectric properties (Section 2.2). Soft computing systems directly utilize data to learn, eliminating the need for predefined equations to identify patterns and trends (Cardoso & Ferreira, 2020; Pourramezan *et al.*, 2024). The backpropagation algorithm (Lillicrap, Cownden, Tweed, & Akerman, 2016) serves as a learning mechanism, providing efficient weight adjustments and achieving low error rates. To enhance the performance of soft computing methods, the dielectric characteristic data are normalized using Equation (3) (Heidari, Rezaei, & Rohani, 2020; Rohani, Abbaspour-Fard, & Abdolahpour, 2011). This normalization technique transforms the data into a range between -1 and 1, ensuring consistency and facilitating the model's training process. Two soft computing models, multilayer perceptron (MLP) and support vector machine (SVM), were employed for this study. Their specific implementation details are described in the subsequent sections.

$$C_N = \frac{(C_i - C_{min})}{(C_{max} - C_{min})} \times (r_{max} - r_{min}) + r_{min} \quad (3)$$

The normalized value (C_N) of each dielectric property is calculated using Equation (3), where C_i represents the original value of the dielectric property, C_{max} and C_{min} represent the maximum and minimum values of the property across all samples, and r_{max} and r_{min} represent the maximum and minimum values considered for the normalized data.

Multilayer perceptron neural network (MLP-NN)

The multilayer perceptron neural network (MLP-NN) comprises an input layer, an output layer, and one hidden layer. In this study, MLP-NN is employed to predict the spectral analysis indices (Fe, Pb, Cu, Al, Mo, Na, Si, and Vis@100) of engine lubricant using the dielectric properties of the oil (ε', ε", tan δ), as illustrated in Figure 4. The input layer is defined based on the correlation analysis of dielectric properties at different frequencies, as shown in Table 2. The output layer represents the desired spectral analysis index of the engine lubricant that we aim to predict. In modeling, the training set constitutes 80% of the dataset, while the testing set accounts for the remaining 20%. The hidden layer incorporates the sigmoid conversion function (Equation 4) (Ashtiani, Rohani, & Aghkhani, 2020; Shi, Song, & Song, 2021).

$$I = \frac{1}{1 + e^{-\sum C_i w_{ij} + b}} \quad (4)$$

where C_i represents the i^{th} input, b denotes the bias factor, and w_{ij} shows the weight of the j^{th} neuron.

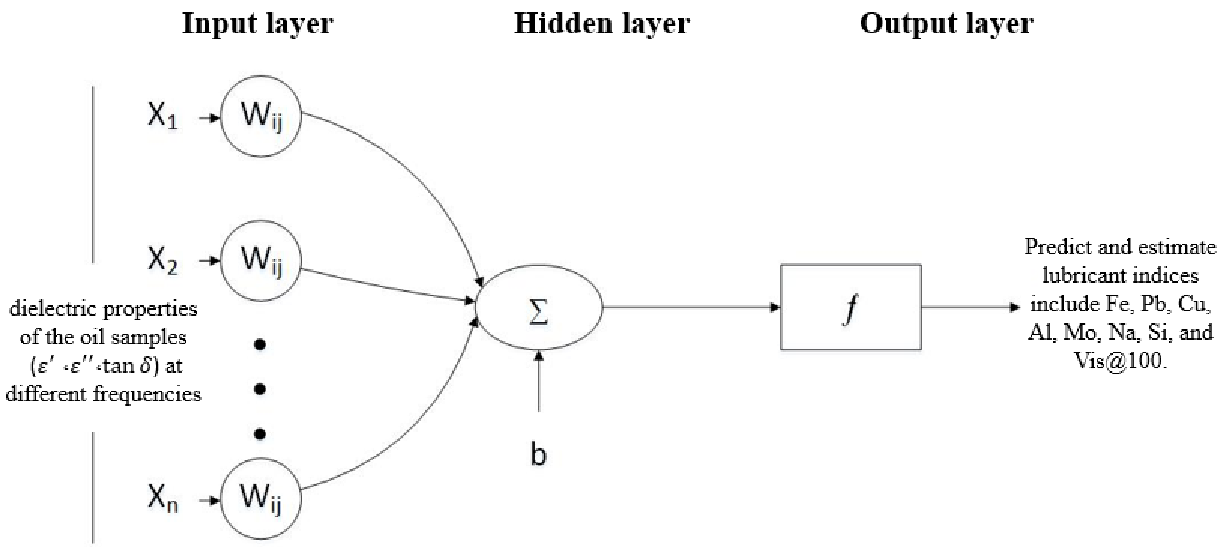

Fig. 4. MLP structure used to predict lubricant indices

Support vector machine (SVM)

Support vector machines (SVMs) were first introduced by Vapnik in the 1990s (Fayazi, Arabloo, Shokrollahi, Zargari, & Ghazanfari, 2014). In this study, SVMs are utilized to predict the spectral analysis indices (Fe, Pb, Cu, Al, Mo, Na, Si, and Vis@100) of engine lubricants based on their dielectric properties (ε', ε", tan δ) at various frequencies (see Fig.5).

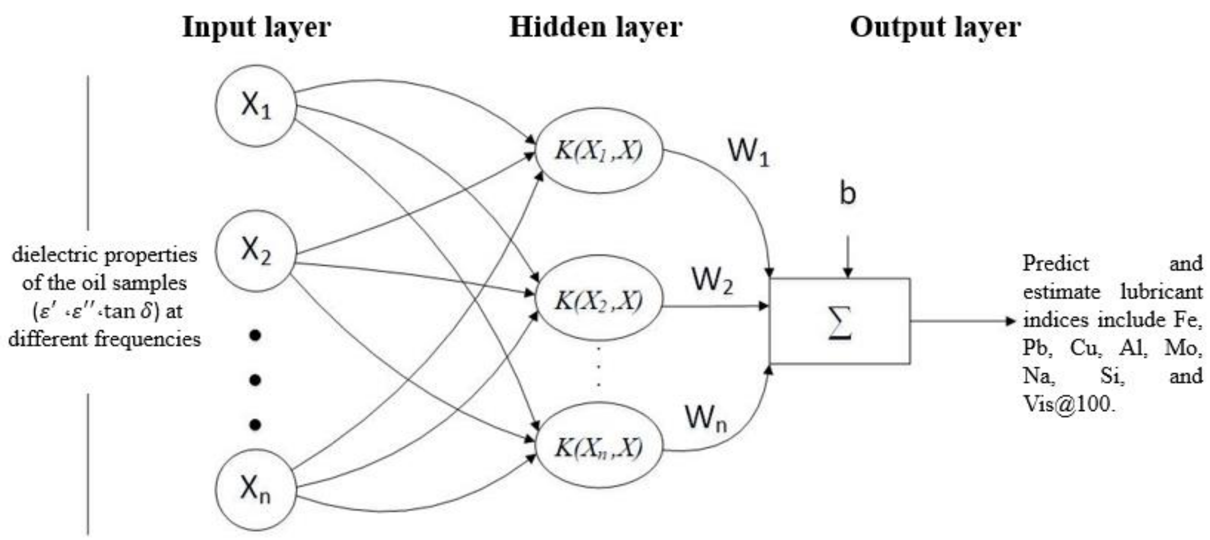

Fig. 5. SVM structure used to predict lubricant indices

Support vector machines (SVMs) are based on statistical learning principles, governed by the following relationships (Chamkalani, Mohammadi, Eslamimanesh, Gharagheizi, & Richon, 2012; Eslamimanesh *et al.*, 2012). The nonlinear function employed in the SVM approach to approximate data sets $\{(X_1, Y_1), (X_2, Y_2), \ldots, (X_n, Y_n)\}$ is given by Equation

(5):

$$f(x) = w\varphi(x) + b \quad (5)$$

where $\varphi(x)$ represents a nonlinear mapping function, w represents the weight vector of the input layer, and b represents the bias factor.

SVM optimization is achieved by minimizing Equation (6) using the Lagrange function (Equation (7)):

$$min_{w,b,e}J(w,e) = \frac{1}{2}\|w\|^2 + \frac{1}{2}\gamma\sum_{i=1}^{n}\xi_i^2 \quad (6)$$

$$s.t. y_i = w.\varphi(x_i) + b + \xi_i, i = 1,2,\dots,n$$

$$L(w,b,\xi,\alpha) = \frac{1}{2}\|w\|^2 + \frac{\gamma}{2}\sum_{i=1}^{n}\xi_i^2 - \sum_{i=1}^{n}\alpha_i\,(w\varphi(x_i) + b + \xi_i - y_i) \quad (7)$$

where ξ_i represents the regression error for n training items, γ is the regularization parameter, α_i is the Lagrange coefficient, and Equation (7) is obtained by considering partial derivatives of w, b, ξ, and α.

Performance evaluation of soft computing models

This study aims to predict spectral analysis indices for engine lubricants based on dielectric properties measured at different frequencies. The performance of the soft computing models, namely MLP and SVM, is assessed using four metrics: root mean square error (RMSE), mean absolute percentage error (MAPE), model efficiency (E), and R-squared (R^2) (Pourramezan, Omidvar, Motavalizadehkakhky, Zhiani, & Darzi, 2024; Pourramezan & Rohani, 2024; Siavash *et al.*, 2021; Soltanali, Rohani, Abbaspour-Fard, & Farinha, 2021):

$$RMSE = \sqrt{\frac{\sum_{i=1}^{n}(y_{pi} - y_{ei})^2}{n}} \quad (8)$$

$$MAPE = \frac{1}{n}\sum_{i=1}^{n}\frac{|y_{pi} - y_{ei}|}{y_{pi}} \quad (9)$$

$$E = \frac{1}{n}\sum_{i=1}^{n}(y_{pi} - y_{ei})^2 \quad (10)$$

$$R^2 = \frac{(\sum_{i=1}^{n}(y_{ei} - \overline{y_{ei}})(y_{pi} - \overline{y_{pi}}))^2}{\sum_{i=0}^{n}(y_{ei} - \overline{y_{ei}})^2\sum_{i=0}^{n}(y_{pi} - \overline{y_{pi}})^2} \quad (11)$$

where y_{pi} and y_{ei} represent the predicting and the measuring indices of engine lubricant spectral analysis, respectively. Here, n represents the number of oil samples.

To assess the performance of the soft computing models, we evaluated the mean, variance, and normal distribution of the predicted values. After comparing the MLP and SVM models, the regression diagram of the predicted and actual values for the superior model was plotted.

Results and Discussion

The optimal frequency for the study was initially identified based on the highest value of the determination coefficient (R^2) (see Fig.6). Subsequently, the ability of dielectric indices (ε', ε'', tan δ) to predict the spectral analysis indices of engine lubricants was examined using soft computing techniques.

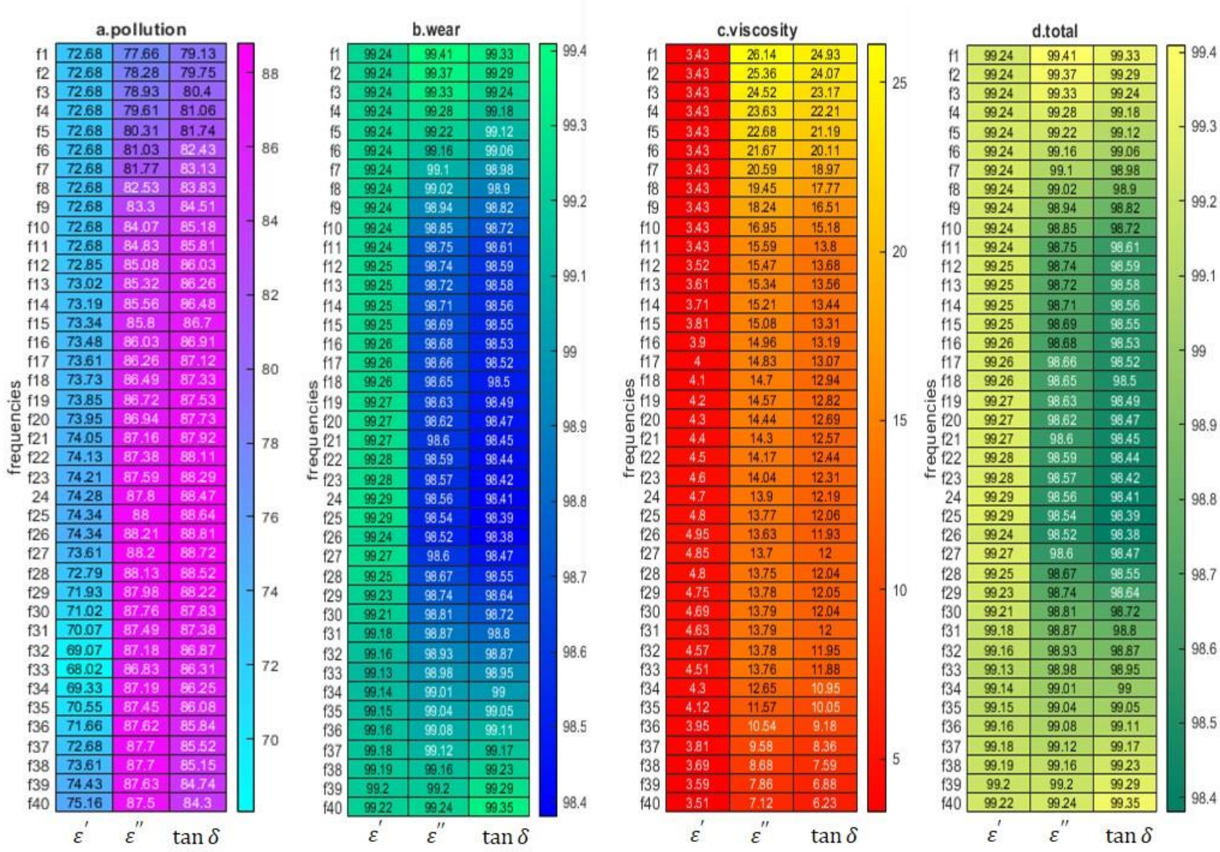

Fig. 6. R^2 of dielectric properties (ε', ε'', $\tan\delta$) at different frequencies (Table 2) by attention to various evaluated lubricant conditions

As depicted in Figure 6, the ε' index exhibited superior performance in the pollution assessment at f40 frequency (R^2 = 75.16) and the viscosity assessment at f40 frequency (R^2= 4.95). However, R^2 = 4.95 is insufficient for reliable prediction. The ε' index also demonstrated exceptional performance in the wear and total assessments at f24 frequency (R^2= 99.29). Additionally, Figure 6 reveals that the ε'' index achieved the highest R^2 value of 88.21 in the pollution assessment at f26 frequency. Furthermore, the ε'' index exhibited the best results in the wear (R^2= 99.41), viscosity (R^2= 26.14), and total assessments at frequency f1, respectively. However, R^2= 26.14 is not sufficiently robust for viscosity prediction. As shown in Figure 6, the $\tan\delta$ index demonstrated exceptional performance in the pollution assessment at f26 frequency (R^2= 88.81) and the viscosity assessment at f1 frequency (R^2= 24.93). While R^2 = 24.93 is insufficient for accurate prediction, the $\tan\delta$ index also achieved the highest R^2 value of 99.35 in the wear and total assessments at f40 frequency.

Setting input parameters for MLP and SVM

As described in the Materials and Methods section, MLP and SVM models were employed to predict the spectral analysis indices of engine lubricants from the measured values of dielectric properties (ε', ε'', $\tan\delta$) at different frequencies. The neural network inputs were determined based on the correlation analysis and expert judgment presented in Table 3.

Table 3- Neural network input parameters for MLP and SVM

Predicted index	Inputs model*
Vis@100	p1, p12, p23, p27, p34, z 1, z2, z27, z34
Si	p12, p27, z1, z2, z12, z34, d 1, d2, d12
Na	p1, p12, p23, p27, p34, z1, z12, z27, z34
Fe	p1, p12, p27, z1, z2, z12, z27, z34, d1, d2, d12, d27
Pb	p1, p12, p15, p16, p23, p27, p28, p34, z1, z2, z12, z27, z30, z34, d1, d2, d3, d12, d24, d25, d26, d27, d35, d39
Cu	z31, z32, z33, z34, z35, z36, z37, z38, z39, d30, d31, d32, d33, d34, d35, d36, d37, d38, d39
Al	p1, p2, p12, p22, p26, p27, p38, z1, z2, z3, z12, z17, z27, z29, z34, d1, d2, d3, d12, d27
Mo	p1, p2, p12, p22, p26, p27, p38, z1, z2, z3, z12, z17, z27, z29, z34, d1, d2, d3, d12, d27

*The p, z, and d are ε', ε'', and $\tan\delta$, respectively. The numeral of each symbol represents the measured frequency point (attention to Table 2).

Comparing the performance of MLP and SVM

In this section, the MLP and SVM models developed in Section 3.1 are evaluated and compared using the performance metrics RMSE, MAPE, and E (Table 4). Generally, smaller values of RMSE and MAPE indicate better model performance, while E values closer to 1 indicate improved model accuracy.

Table 4- Comparative performance of the SVM and MLP models

Predicted index	Phase	SVM			MLP		
		RMSE	MAPE	E	RMSE	MAPE	E
Vis@100	Train	0.23	1.2	0.99	0.38	1.91	0.98
	Test	0.49	2.74	0.96	0.49	1.99	0.96
	Total	0.3	1.5	0.99	0.41	1.93	0.97
Si	Train	0.74	-	0.99	0.5	-	0.99
	Test	1	-	0.99	1.5	-	0.97
	Total	0.8	-	0.99	0.8	-	0.99
Na	Train	0.43	-	0.98	0.69	-	0.96
	Test	0.52	-	0.98	0.93	-	0.92
	Total	0.45	-	0.98	0.75	-	0.95
Fe	Train	1.88	-	0.99	5.83	-	0.92
	Test	4.44	-	0.95	5	-	0.93
	Total	2.59	-	0.98	5.67	-	0.93
Pb	Train	0.21	-	0.98	0.99	-	0.61
	Test	0.46	-	0.91	0.82	-	0.71
	Total	0.28	-	0.97	0.96	-	0.62
Cu	Train	0.34	-	0.96	0.57	-	0.88
	Test	0.46	-	0.96	0.97	-	0.81
	Total	0.37	-	0.96	0.67	-	0.86
Al	Train	0.65	-	0.99	2.38	-	0.86
	Test	1.16	-	0.98	2.09	-	0.94
	Total	0.78	-	0.99	2.32	-	0.89
Mo	Train	1.05	-	0.99	7.25	-	0.82
	Test	1.84	-	0.98	5.47	-	0.82
	Total	1.24	-	0.99	6.94	-	0.82

Table 4 presents the performance of the MLP and SVM models in predicting the spectral analysis indices of engine lubricants. The results indicate that the SVM model consistently exhibits superior performance across all indices, as evidenced by its higher E values and lower RMSE scores. For instance, in the prediction of iron content, the SVM model achieved an E value of 0.98 and an RMSE of 2.59, compared to the MLP model's

0.93 and 5.67, respectively. Similarly, Table 5 compares the MLP and SVM models based on the mean, variance, and normal distribution of the predicted values, confirming the SVM model's superior modeling capabilities. Figure 7 depicts the coefficient of determination (R^2) between the actual and predicted values of the spectral analysis indices. The R^2 values for both training and testing stages demonstrate that the SVM model closely aligns the actual and predicted values. This is further evident from the slopes of the regression lines, which approach unity and zero in the SVM model. Consequently, the SVM model successfully predicts the values of most spectral analysis indices with a high degree of accuracy, achieving an R^2 value of approximately 0.99.

Table 5- Evaluating MLP and SVM models by mean, variance, and normal distribution

Predicted index	Phase	SVM			MLP		
		Mean	Variance	Distribution	Mean	Variance	Distribution
Vis@100	Train	0.95	0.83	0.99	0.83	0.98	0.9
	Test	0.82	0.92	0.11	0.81	0.99	0.11
	Total	0.96	0.86	0.69	0.76	0.99	0.69
Si	Train	0.98	0.85	0.55	0.99	0.99	0.99
	Test	0.92	0.86	0.97	0.99	0.99	0.97
	Total	0.95	0.91	0.37	0.99	0.98	0.96
Na	Train	0.93	0.72	0.55	0.99	0.85	0.9
	Test	0.9	0.89	0.97	0.77	0.99	0.68
	Total	0.89	0.7	0.52	0.89	0.86	0.52
Fe	Train	0.94	0.79	0.9	0.98	0.74	0.99
	Test	0.99	0.71	0.97	0.97	0.94	0.97
	Total	0.94	0.69	0.85	0.99	0.74	0.96
Pb	Train	0.94	0.53	0	0.49	0	0.01
	Test	0.72	0.47	0.31	0.54	0.52	0.68
	Total	0.83	0.39	0	0.36	0	0
Cu	Train	0.94	0.67	0.55	0.71	0.51	0.74
	Test	0.99	0.88	0.97	0.94	0.95	0.97
	Total	0.96	0.65	0.52	0.72	0.65	0.69
Al	Train	0.97	0.85	0.94	0.46	0.08	0.09
	Test	0.74	0.99	0.77	0.8	0.97	0.97
	Total	0.55	0.97	0.52	0.46	0.22	0.06
Mo	Train	0.95	0.81	0.74	0.86	0.15	0.55
	Test	0.95	0.89	0.31	0.85	0.2	0.97
	Total	0.94	0.78	0.37	0.82	0.08	0.52

Sensitivity analysis

The SVM model demonstrated superior performance in predicting the spectral analysis indices of engine lubricants, as evidenced by its higher E values, lower RMSE scores, and closer alignment of actual and predicted values (Tables 4 and 5). Further analysis revealed that the SVM model's regression line closely approximates unity and zero, indicating a high degree of accuracy. Sensitivity analysis plays a crucial role in model development and application by identifying the most influential parameters and simplifying the model (Glagolev, 2012). It enables the assessment of how changes in input parameters affect the model's output (Iooss & Lemaître, 2015). In this study, sensitivity analysis was employed to evaluate the importance of each dielectric index value in predicting the spectral analysis indices of engine lubricants. RMSE was used as the criterion for assessing sensitivity. Therefore, if removing an input increases RMSE, it indicates its significance (RMSE should approach zero). Conversely, if removing an input reduces RMSE, it suggests its lower importance (Chaudhry, Buchwald, &

Nagel, 2021; Rezaei, Rohani, Heidari, & Lawson, 2021). Figure 8 illustrates the results of sensitivity analysis conducted by the SVM model to predict the spectral analysis parameters of engine lubricants.

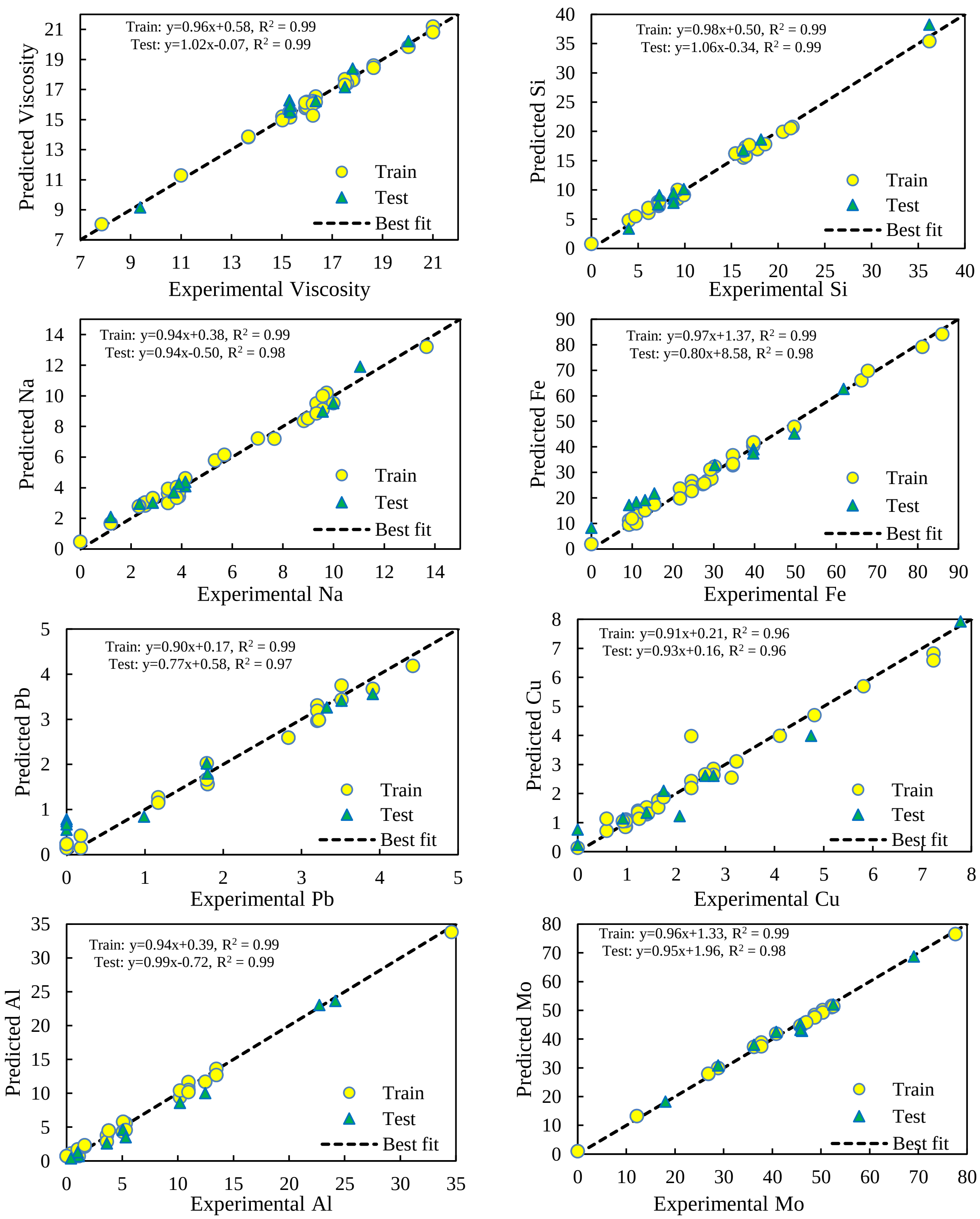

Fig. 7. Comparison of experimental and predicted lubricant spectral analysis (SA) indexes using the SVM model

The sensitivity analysis results for predicting viscosity revealed that removing inputs z27, p23, p27, and z34 resulted in increased RMSE, indicating their higher significance. Conversely, removing inputs p34, z1, and z27 did not significantly impact RMSE. Removing inputs p1 and p12 led to reduced RMSE, implying their lower significance. Three models with reduced inputs were subsequently proposed; however, none improved RMSE. The sensitivity analysis for predicting silicon indicated that removing inputs p12, p27, d12, and z34 increased RMSE, while eliminating inputs d1, d2, z1, z2, and z12 reduced RMSE. Two models with limited inputs were proposed, and one (p12, p27, z34, d1, and d12) achieved improved RMSE. Sensitivity analysis for predicting sodium showed that removing inputs z27 and p34 increased RMSE, while removing inputs p1, p12, p27, and z12 had no significant impact. Removing inputs p23, z1, and z34 decreased RMSE, suggesting their lower significance. One model (p1, p12, p27, p34, z12, and z27) was proposed and successfully improved RMSE. Iron prediction sensitivity analysis revealed that removing inputs p27, d27, and d1 resulted in increased RMSE, while removing inputs z12, z27, z34, p1, p12, z1, d2, d12, and z2 reduced RMSE. One model (z12, z27, z34, p1, p12, p27, d1, and d27) was suggested and improved RMSE. Lead prediction sensitivity analysis indicated that removing inputs d25, z1, d27, d39, d15, z12, d12, z27, p1, d2, d3, z2, p12, p16, p27, p34, d1, p28, d26, z34, d24, d35, and p23 led to increased RMSE, while removing input z30 reduced RMSE. No model with limited inputs improved RMSE. The sensitivity analysis for predicting copper revealed that removing inputs d39, z35, d31, z36, z39, and d33 increased RMSE, while removing input d38 did not affect RMSE and removing inputs d32, d35, z32, z33, z37, z38, d30, d36, d37, z31, z34, and z35 decreased RMSE. One model (d39, z35, d31, z36, z39, d33, d38, d32, and d35) was proposed and successfully improved RMSE.

The sensitivity analysis for predicting aluminum revealed that removing inputs d12, d3, z3, z27, z17, d2, z29, z34, and d27 led to increased RMSE, indicating their higher significance. Conversely, removing inputs p1, p2, p12, p22, p26, p27, z1, z2, z12, and d1 had no significant impact on RMSE. Removing input p38 resulted in reduced RMSE, suggesting its lower significance. A model with the reduced inputs (d12, d3, z3, z27, z17, d2, z29, z34, d27, and p1) was proposed and successfully improved RMSE. Molybdenum prediction sensitivity analysis indicated that removing inputs z27, z12, z34, z17, d3, z2, p38, z1, p2, d12, p12, p1, z29, d27, d2, z3, and d1 led to increased RMSE, while removing inputs p27, p22, and p26 resulted in reduced RMSE. No model with limited inputs improved RMSE.

Building upon the insights gained from sensitivity analysis, the final models for predicting the viscosity, Si, Na, Fe, Pb, Cu, Mo, and Al values of engine lubricant using SVM were proposed. While models with fewer inputs were considered for viscosity prediction, none of them could significantly enhance the RMSE. For Si prediction, a model with reduced inputs was proposed, and it successfully improved RMSE. Similarly, models with less significant inputs were identified for Na and Fe predictions, leading to improved RMSE values. In contrast, a model with more significant inputs was developed for Pb prediction, but it failed to improve RMSE. For Cu and Al prediction, models with less significant inputs were found, and they effectively reduced RMSE. Overall, the final models exhibit promising accuracy, as RMSE improvements were achieved by eliminating less influential inputs.

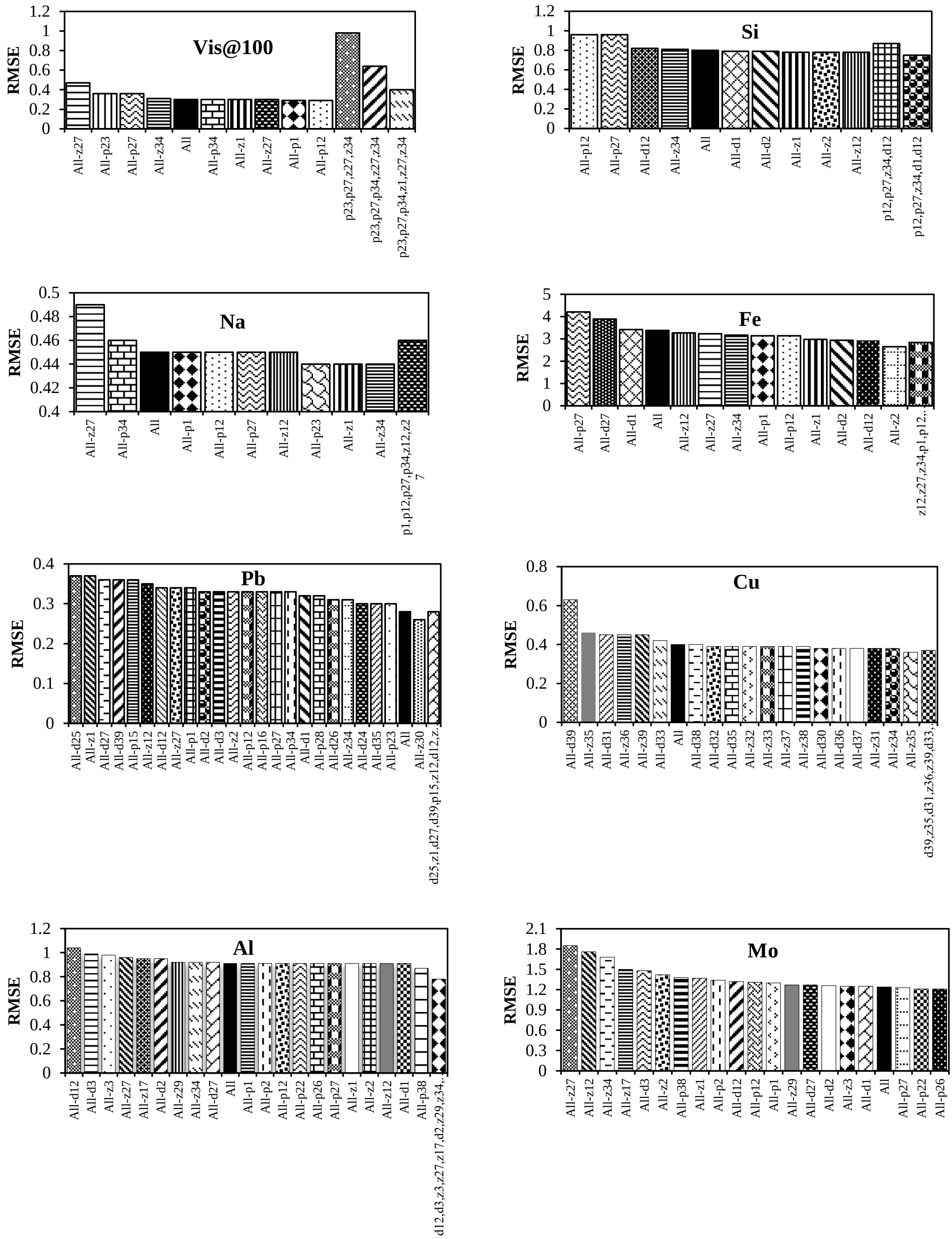

Fig. 8. Result of sensitivity analysis (attention to Table 3)

Conclusion

This study investigated the dielectric properties (ε', ε'', tan δ) of 17 lubricant samples, including 16 used oil samples and one fresh oil sample. Dielectric measurements were performed at 40 frequencies ranging from 300 MHz to 9 GHz. Initially, the correlation between dielectric properties and lubricant conditions was analyzed in four evaluation categories: pollution, erosion, viscosity, and general. The dielectric constant (ε') index exhibited the highest coefficient of determination (R2) for pollution at frequencies f40, f24, and f26, and for erosion, viscosity, and general at frequencies f26, f40, f1, and f40, respectively. The dielectric loss tangent (tan δ) index displayed the strongest correlation with pollution at frequency f27 and with erosion, viscosity, and general at frequencies f1, f26, and f40, respectively. Subsequently, multilayer perceptron (MLP) and support vector machine (SVM) models were designed to predict the spectral analysis indices of engine lubricants based on dielectric properties. The inputs for these models were determined using correlation and speculation analyses. The performance of the models was evaluated and compared using three metrics: root mean squared error (RMSE), mean absolute percentage error (MAPE), and efficiency (E). The SVM model outperformed the MLP model and was selected as the preferred model for predicting lubricant condition indices. Sensitivity analysis was employed to assess the importance of each model input. The findings of this study demonstrate that soft computing techniques can effectively estimate the spectral analysis indices of engine lubricants (Fe, Pb, Cu, Al, Mo, Na, Si, and Vis@100) using their dielectric properties (ε', ε'', tan δ). This approach offers a promising and practical method for monitoring the condition of diesel engine lubricants, particularly for off-road machinery operating in remote areas with limited access to oil analysis laboratories. The SVM model achieved an efficiency score exceeding 0.95 for all predicted indices, highlighting its potential for real-world applications. While the limited sample size somewhat restricts the scope of this research, the results provide a strong proof-of-concept and pave the way for further validation on an industrial scale. Despite the potential for online and portable equipment implementation, the study's laboratory setting under controlled conditions raises concerns about the accuracy and consistency of input data in real-world scenarios. Therefore, further research involving a larger statistical population and a broader range of lubricant types is necessary to fully assess the comprehensiveness and commercialization potential of this method. The accuracy of predictions based on electrical properties may depend on the quality and consistency of the input data, emphasizing the need for rigorous validation in field conditions.

Acknowledgment

We gratefully acknowledge the financial support provided by Ferdowsi University of Mashhad in Iran for this research project. We also appreciate the valuable contribution of Tirage Company for granting us access to their maintenance database.

Conflicts of interest

The authors have no conflicts of interest to disclose.

Compliance with Ethical Standards

This work does not contain any studies with human participants or animals performed by any of the authors.

Funding

This research was supported by Ferdowsi University of Mashhad in Iran (Grant number 59252).

Authors Contribution

M. R. Pourramezan: Conceptualization, Investigation, Software, Formal analysis, Writing-original draft.

A. Rohan: Funding acquisition, Software, Formal analysis, Project administration, Supervision, and Validation.

M. H. Abbaspour-Fard: Advisor,

Supervision, Validation, Writing-review & editing

Data Availability

The datasets analyzed during the current study are not publicly available but are available from the corresponding author on reasonable request.

References

1. Altıntaş, O., Aksoy, M., Ünal, E., Akgöl, O., & Karaaslan, M. (2019). Artificial neural network approach for locomotive maintenance by monitoring dielectric properties of engine lubricant. *Measurement*, *145*, 678-686. https://doi.org/10.1016/j.measurement.2019.05.087
2. Ashtiani, S.-H. M., Rohani, A., & Aghkhani, M. H. (2020). Soft computing-based method for estimation of almond kernel mass from its shell features. *Scientia Horticulturae*, *262*, 109071. https://doi.org/10.1016/j.scienta.2019.109071
3. Bhattacharya, A., & Dan, P. K. (2014). Recent trend in condition monitoring for equipment fault diagnosis. *International Journal of System Assurance Engineering and Management*, *5*, 230-244. https://doi.org/10.1007/s13198-013-0151-z
4. Cardoso, D., & Ferreira, L. (2020). Application of predictive maintenance concepts using artificial intelligence tools. *Applied Sciences*, *11*(1), 18. https://doi.org/10.3390/app11010018
5. Chamkalani, A., Mohammadi, A. H., Eslamimanesh, A., Gharagheizi, F., & Richon, D. (2012). Diagnosis of asphaltene stability in crude oil through “two parameters” SVM model. *Chemical Engineering Science*, *81*, 202-208. https://doi.org/10.1016/j.ces.2012.06.060
6. Chaudhry, A. A., Buchwald, J., & Nagel, T. (2021). Local and global spatio-temporal sensitivity analysis of thermal consolidation around a point heat source. *International Journal of Rock Mechanics and Mining Sciences*, *139*, 104662. https://doi.org/10.1016/j.ijrmms.2021.104662
7. Chun, S.-M. (2006). Study on Mutual Relation between the Level of Deterioration Influenced by the Changes of Chemical and Physical Properties and the Change of Dielectric Constant for Engine Oil-Diesel Engine Oil. *Tribology and Lubricants*, *22*(5), 290-300. https://doi.org/10.9725/kstle.2006.22.5.290
8. Duchowski, J. K., & Mannebach, H. (2006). A novel approach to predictive maintenance: a portable, multi-component MEMS sensor for on-line monitoring of fluid condition in hydraulic and lubricating systems. *Tribology Transactions*, *49*(4), 545-553. https://doi.org/10.1080/10402000600885183
9. Eslamimanesh, A., Gharagheizi, F., Illbeigi, M., Mohammadi, A. H., Fazlali, A., & Richon, D. (2012). Phase equilibrium modeling of clathrate hydrates of methane, carbon dioxide, nitrogen, and hydrogen+ water soluble organic promoters using Support Vector Machine algorithm. *Fluid Phase Equilibria*, *316*, 34-45. https://doi.org/10.1016/j.fluid.2011.11.029
10. Fayazi, A., Arabloo, M., Shokrollahi, A., Zargari, M. H., & Ghazanfari, M. H. (2014). State-of-the-art least square support vector machine application for accurate determination of natural gas viscosity. *Industrial & Engineering Chemistry Research*, *53*(2), 945-958. https://doi.org/10.1021/ie402829p
11. Gerhardt, R. A. (2022). What is Impedance and Dielectric Spectroscopy? *IEEE Instrumentation & Measurement Magazine*, *25*(4), 14-20. https://doi.org/10.1109/MIM.2022.9777776
12. Glagolev, M. (2012). Sensitivity analysis of the model. *Environmental Dynamics and Global Climate Change*, *3*(3), 31-53. https://doi.org/10.17816/edgcc3331-53
13. Gomółka, L., & Augustynowicz, A. (2019). Evaluation of applicability of dielectric constant in monitoring aging processes in engine oils. *Eksploatacja i Niezawodność*, *21*(2), 177-185. https://doi.org/10.17531/ein.2019.2.1
14. Guan, L., Feng, X., Xiong, G., & Xie, J. (2011). Application of dielectric spectroscopy for engine lubricating oil degradation monitoring. *Sensors and Actuators A: Physical*, *168*(1), 22-

29. https://doi.org/10.1016/j.sna.2011.03.033
15. Heidari, P., Rezaei, M., & Rohani, A. (2020). Soft computing-based approach on prediction promising pistachio seedling base on leaf characteristics. *Scientia Horticulturae*, *274*, 109647. https://doi.org/10.1016/j.scienta.2020.109647
16. Heredia-Cancino, J., Ramezani, M., & Álvarez-Ramos, M. (2018). Effect of degradation on tribological performance of engine lubricants at elevated temperatures. *Tribology International*, *124*, 230-237. https://doi.org/10.1016/j.triboint.2018.04.015
17. Hong, S.-H., & Jeon, H.-G. (2022). Monitoring the conditions of hydraulic oil with integrated oil sensors in construction equipment. *Lubricants*, *10*(11), 278. https://doi.org/10.3390/lubricants10110278
18. Iooss, B., & Lemaître, P. (2015). A review on global sensitivity analysis methods. *Uncertainty management in simulation-optimization of complex systems: algorithms and applications*, 101-122. https://doi.org/10.1007/978-1-4899-7547-8_5
19. Kim, H.-J., Seo, K.-J., Kang, K. H., & Kim, D.-E. (2016). Nano-lubrication: A review. *International Journal of Precision Engineering and Manufacturing*, *17*, 829-841. https://doi.org/10.1007/s12541-016-0102-0
20. Król, A., Gocman, K., & Giemza, B. (2015). Neural networks as a tool to characterise oil state after porous bearings prolonged tests. *Materials Science*, *21*(3), 466-472. https://doi.org/10.5755/j01.ms.21.3.7506
21. Lazakis, I., Raptodimos, Y., & Varelas, T. (2018). Predicting ship machinery system condition through analytical reliability tools and artificial neural networks. *Ocean Engineering*, *152*, 404-415. https://doi.org/10.1016/j.oceaneng.2017.11.017
22. Li, L., Chang, W., Zhou, S., & Xiao, Y. (2017). *An identification and prediction model of wear-out fault based on oil monitoring data using PSO-SVM method.* Paper presented at the 2017 Annual Reliability and Maintainability Symposium (RAMS). https://doi.org/10.1109/RAM.2017.7889670
23. Li, Z., Fei, F., & Zhang, G. (2022). Edge-to-Cloud IIoT for Condition Monitoring in Manufacturing Systems with Ubiquitous Smart Sensors. *Sensors*, *22*(15), 5901. https://doi.org/10.3390/s22155901
24. Lillicrap, T. P., Cownden, D., Tweed, D. B., & Akerman, C. J. (2016). Random synaptic feedback weights support error backpropagation for deep learning. *Nature communications*, *7*(1), 13276. https://doi.org/10.1038/ncomms13276
25. Macián, V., Tormos, B., Olmeda, P., & Montoro, L. (2003). Analytical approach to wear rate determination for internal combustion engine condition monitoring based on oil analysis. *Tribology International*, *36*(10), 771-776. https://doi.org/10.1016/S0301-679X(03)00060-4
26. Mondelin, A., Claudin, C., Rech, J., & Dumont, F. (2011). Effects of lubrication mode on friction and heat partition coefficients at the tool–work material interface in machining. *Tribology Transactions*, *54*(2), 247-255. https://doi.org/10.1080/10402004.2010.538489
27. Mosher, P. (2007). Predicting failure–condition monitoring in action. *World Pumps*, *2007*(484), 24-28. https://doi.org/10.1016/S0262-1762(06)71208-1
28. Mumby, S. J. (1989). An overview of laminate materials with enhanced dielectric properties. *Journal of Electronic Materials*, *18*(2), 241-250. https://doi.org/10.1007/BF02657415
29. Newell, G. E. (1999). Oil analysis cost-effective machine condition monitoring technique. *Industrial Lubrication and tribology*, *51*(3), 119-124. https://doi.org/10.1108/00368799910268066
30. Nüchter, M., Ondruschka, B., Bonrath, W., & Gum, A. (2004). Microwave assisted synthesis–a critical technology overview. *Green Chemistry*, *6*(3), 128-141. https://doi.org/10.1039/B310502D
31. Pourramezan, E., Omidvar, M., Motavalizadehkakhky, A., Zhiani, R., & Darzi, H. H. (2024).

Enhanced adsorptive removal of methylene blue using ternary nanometal oxides in an aqueous solution. *Biomass Conversion and Biorefinery*, 1-13. https://doi.org/10.1007/s13399-023-05225-2
32. Pourramezan, M.-R., & Rohani, A. (2024). Improved Monitoring and Classification of Engine Oil Condition through Two Machine Learning Techniques. *SAE International Journal of Fuels and Lubricants, 18*(04-18-01-0005). https://doi.org/10.4271/04-18-01-0005
33. Pourramezan, M.-R., Rohani, A., & Abbaspour-Fard, M. H. (2023a). Comparative Analysis of Soft Computing Models for Predicting Viscosity in Diesel Engine Lubricants: An Alternative Approach to Condition Monitoring. *ACS omega*. https://doi.org/10.1021/acsomega.3c07780
34. Pourramezan, M.-R., Rohani, A., & Abbaspour-Fard, M. H. (2023b). Unlocking the Potential of Soft Computing for Predicting Lubricant Elemental Spectroscopy. *Lubricants*, *11*(9), 382. https://doi.org/10.3390/lubricants11090382
35. Pourramezan, M.-R., Rohani, A., & Abbaspour-Fard, M. H. (2024). Machine Learning-Based Predictions of Metal and Non-Metal Elements in Engine Oil Using Electrical Properties. *Lubricants*, *12*(12), 411. https://doi.org/10.3390/lubricants12120411
36. Pourramezan, M.-R., Rohani, A., & Abbaspour-Fard, M. H. (2025). Comprehensive Review of Dielectric, Impedance, and Soft Computing Techniques for Lubricant Condition Monitoring and Predictive Maintenance in Diesel Engines. *Lubricants*, *13*(8), 328. https://doi.org/10.3390/lubricants13080328
37. Pourramezan, M.-R., Rohani, A., Keramat Siavash, N., & Zarein, M. (2022). Evaluation of lubricant condition and engine health based on soft computing methods. *Neural Computing and Applications*, 1-13. https://doi.org/10.1007/s00521-021-06688-y
38. Raadnui, S., & Kleesuwan, S. (2005). Low-cost condition monitoring sensor for used oil analysis. *Wear*, *259*(7-12), 1502-1506. https://doi.org/10.1016/j.wear.2004.11.009
39. Rahimi, M., Pourramezan, M.-R., & Rohani, A. (2022). Modeling and classifying the in-operando effects of wear and metal contaminations of lubricating oil on diesel engine: A machine learning approach. *Expert Systems with Applications*, *203*, 117494. https://doi.org/10.1016/j.eswa.2022.117494
40. Rezaei, M., Rohani, A., Heidari, P., & Lawson, S. (2021). Using soft computing and leaf dimensions to determine sex in immature Pistacia vera genotypes. *Measurement*, *174*, 108988. https://doi.org/10.1016/j.measurement.2021.108988
41. Rohani, A., Abbaspour-Fard, M. H., & Abdolahpour, S. (2011). Prediction of tractor repair and maintenance costs using Artificial Neural Network. *Expert Systems with Applications*, *38*(7), 8999-9007. https://doi.org/10.1016/j.eswa.2011.01.118
42. Sangha, M. S., Gomm, J. B., & Yu, D. (2008). Neural network fault classification of transient data in an automotive engine air path. *International Journal of Modelling, Identification and Control, 3*(2), 148-155. https://doi.org/10.1504/IJMIC.2008.019352
43. Sapotta, B., Schwotzer, M., Wöll, C., & Franzreb, M. (2022). On the Integration of Dielectrometry into Electrochemical Impedance Spectroscopy to Obtain Characteristic Properties of a Dielectric Thin Film. *Electroanalysis*, *34*(3), 512-522. https://doi.org/10.1002/elan.202100484
44. Shi, Y., Song, X., & Song, G. (2021). Productivity prediction of a multilateral-well geothermal system based on a long short-term memory and multi-layer perceptron combinational neural network. *Applied Energy*, *282*, 116046. https://doi.org/10.1016/j.apenergy.2020.116046
45. Siavash, N. K., Ghobadian, B., Najafi, G., Rohani, A., Tavakoli, T., Mahmoodi, E., & Mamat, R. (2021). Prediction of power generation and rotor angular speed of a small wind turbine equipped to a controllable duct using artificial neural network and multiple linear regression. *Environmental Research*, *196*, 110434. https://doi.org/10.1016/j.envres.2020.110434
46. Soltanali, H., Rohani, A., Abbaspour-Fard, M. H., & Farinha, J. T. (2021). A comparative study

of statistical and soft computing techniques for reliability prediction of automotive manufacturing. *Applied Soft Computing*, *98*, 106738. https://doi.org/10.1016/j.asoc.2020.106738

47. Woodley, B. (1978). Failure prediction by condition monitoring (part 1). *International Journal of Materials in Engineering Applications*, *1*(1), 19-26. https://doi.org/10.1016/0141-5530(78)90004-3
48. You, M., Liu, F., & Meng, G. (2011). Benefits from condition monitoring techniques: a case study on maintenance scheduling of ball grid array solder joints. *Proceedings of the Institution of Mechanical Engineers, Part E: Journal of Process Mechanical Engineering*, *225*(3), 205-215. https://doi.org/10.1177/2041300910393426
49. Yu, S., Zhao, D., Chen, W., & Hou, H. (2016). Oil-immersed power transformer internal fault diagnosis research based on probabilistic neural network. *Procedia Computer Science*, *83*, 1327-1331. https://doi.org/10.1016/j.procs.2016.04.276
50. Zarein, M., Khoshtaghaza, M. H., & Ameri Mahabadi, H. (2019). Dielectric Properties of Castor-based Biodiesel Using Microwave. *Fuel and Combustion*, *12*(1), 1-12. https://doi.org/10.22034/jfnc.2019.87991
51. Zeng, Y., Zhang, H., Zhang, H., & Hu, Z. (2010). Effective permittivity calculation of composites with interpenetrating phases. *Journal of Electronic Materials*, *39*, 1351-1357. https://doi.org/10.1007/s11664-010-1229-x
52. Zhu, B., Wang, X., Luo, L., Zhang, N., & Liu, X. (2022). Influence of lubricant supply on thermal and efficient performances of a gear reducer for electric vehicles. *Journal of Tribology*, *144*(1), 011202. https://doi.org/10.1115/1.4052681
53. Zhu, X., Zhong, C., & Zhe, J. (2017). Lubricating oil conditioning sensors for online machine health monitoring–A review. *Tribology International*, *109*, 473-484. https://doi.org/10.1016/j.triboint.2017.01.015
54. Zzeyani, S., Mikou, M., & Naja, J. (2018). Physicochemical Characterization of the Synthetic Lubricating Oils Degradation under the Effect of Vehicle Engine Operation. *Eurasian Journal of Analytical Chemistry*, *13*(4). https://doi.org/10.29333/ejac/90761

ارزیابی ویسکوزیته و سطوح آلاینده در روان‌کننده دیزل از طریق طیف‌سنجی دی‌الکتریک با استفاده از روش‌های محاسباتی نرم

محمدرضا پوررمضان[۱]، عباس روحانی[۱*]، محمدحسین عباسپورفرد[۱]

تاریخ دریافت: ۱۴۰۳/۱۱/۰۵
تاریخ پذیرش: ۱۴۰۴/۰۱/۱۷

چکیده

نظارت بر وضعیت ماشین‌آلات یکی از جنبه‌های حیاتی واحدهای تولیدی و خدماتی برای حفظ کارایی عملیاتی است. از این رو، تعویض به‌موقع روغن موتور به‌طور قابل‌توجهی به افزایش عملکرد و افزایش طول عمر موتور کمک می‌کند. با این حال، تعیین زمان دقیق تعویض همچنان یک چالش است. آنالیز طیفی روغن، در عین این‌که موثر است، هم گران و هم زمان‌بر است. هدف این مطالعه معرفی یک روش جایگزین برای تحلیل طیفی روانکار موتور است. این تحقیق شامل تجزیه و تحلیل نتایج تجزیه و تحلیل طیفی و ضرایب دی‌الکتریک ۱۷ نمونه روغن موتور از طریق روش‌های آماری است. هدف اصلی توسعه مدل‌هایی برای پیش‌بینی آلاینده‌های موجود در روغن بر اساس خواص دی‌الکتریک است که جایگزینی برای تجزیه و تحلیل طیفی ارائه می‌دهد. برای رسیدن به این هدف چند هدف میانی دنبال می‌شود. شبکه عصبی مصنوعی پرسپترون چندلایه (MLP-ANN) و روش ماشین بردار پشتیبان (SVM) برای مدل‌سازی استفاده می‌شوند. عملکرد دو مدل با استفاده از شاخص‌هایی مانند ریشه میانگین مربعات خطا (RMSE)، کارایی مدل و ضریب تبیین (R^2) ارزیابی می‌شود. نتایج نشان می‌دهد که مدل SVM به‌طور مداوم کارایی بیش از ۰/۹۵ را برای همه شاخص‌های پیش‌بینی‌شده (Fe، Pb، Cu، Al، Mo، Na، Si و Vis@100) نشان می‌دهد. در نتیجه، طیف‌سنجی دی‌الکتریک روان‌کننده به‌عنوان یک جایگزین مناسب برای آنالیز مرسوم طیفی روغن متصور می‌باشد.

واژه های کلیدی: ثابت دی‌الکتریک، روش‌های محاسبات نرم، مترولوژی، نظارت بر وضعیت روغن موتور

۱- گروه مهندسی بیوسیستم، دانشکده کشاورزی، دانشگاه فردوسی مشهد، مشهد، ایران
(*- نویسنده مسئول: Email: arohani@um.ac.ir)

https://doi.org/10.22067/jam.2025.91756.1335